Signal Processing 93 (2013) 2003–2009

Contents lists available at SciVerse ScienceDirect

Signal Processing

journal homepage: www.elsevier.com/locate/sigpro

Multi-SVD based subspace estimation to improve angle estimation accuracy in bistatic MIMO radar

Yuanbing Cheng [a,*,1], Rusheng Yu [a,b], Hong Gu [a], Weimin Su [a]

[a] Department of Electronic Engineering and Optoelectronic Technology, Nanjing University of Science and Technology, Nanjing, Jiangsu 210094, China
[b] NARI Technology Development Limited Company, Nanjing, Jiangsu 210061, China

ARTICLE INFO

Article history:
Received 16 April 2012
Received in revised form
17 October 2012
Accepted 28 December 2012
Available online 8 January 2013

Keywords:
Bistatic MIMO radar
Angle estimation
Multi-SVD
Subspace

ABSTRACT

A new multi-SVD based subspace estimation algorithm is proposed to improve the direction of departure (DOD) and direction of arrival (DOA) estimation accuracy for bistatic multiple-input multiple-output (MIMO) radar. First, the matched filter output is transformed to a 3-order tensor. Then the signal subspace is estimated by multi-SVD of the matrix unfoldings of this tensor or its covariance tensor. Since the multidimensional structure is utilized, the estimated signal subspace of our method has better accuracy than that of the traditional SVD/EVD method. Combined with the classical subspace based methods, such as MUSIC and ESPRIT, the proposed approach improves the angle estimation performance compared with the existing ones. Simulation results confirm the effectiveness of our method.

1. Introduction

Multiple-input multiple-output (MIMO) radar has gained increasing attention and becomes a hot research area for its potential advantages [1–3]. It utilizes multiple antennas to simultaneously transmit several orthogonal waveforms and receive reflected signals in similar ways. According to the configuration of transmit/receive arrays, two kinds of MIMO radars are formed. One is called statistical MIMO radar [1], which can resist the radar cross section (RCS) scintillation effect due to the widely spaced transmit antennas and receive antennas. The other one is named co-located MIMO radar [2], including monostatic and bistatic cases, whose elements in transmit and receive arrays are closely spaced. In co-located MIMO radar, one can obtain virtual aperture in the receiver which is larger than the real one through waveform diversity. This yields many advantages such as flexible spatial transmit beam pattern design and high resolution spatial spectral estimation [2,3].

Direction of arrival estimation is encountered in a variety of signal processing applications including radar [4] and communications [5,6]. In bistatic MIMO radar, direction of departure (DOD) and direction of arrival (DOA) estimation is a key issue, and several approaches have been studied [7–14]. A two-dimensional (2-D) capon based spectrum searching method is presented in [7]. 2-D MUSIC and reduced-dimension MUSIC (RD-MUSIC) are discussed in [8], and the latter has lower computational cost but a little performance loss than the former. The above schemes all need spectrum peak searching, which costs significantly. To lower computational cost, ESPRIT is applied [9–12]. In [9], DOD and DOA are estimated through two independent 1-D ESPRITs, but an additional pair matching operation is required. An automatically paired DOD–DOA estimation approach utilizing the inter-relationship between the two 1-D ESPRITs is proposed in [10]. Jin et al. [11] proposed an ESPRIT based method, but the number of transmit antennas is limited to two or three. By dividing the transmit array into two subarrays,

* Corresponding author. Tel./fax: +86 25 84315434.
E-mail address: chengyb@yeah.net (Y. Cheng).
[1] Postal address: Department of Electronic Engineering and Optoelectronic Technology, Nanjing University of Science and Technology, Room 447, Nanjing, Jiangsu 210094, China.

0165-1684/$ - see front matter
http://dx.doi.org/10.1016/j.sigpro.2012.12.021

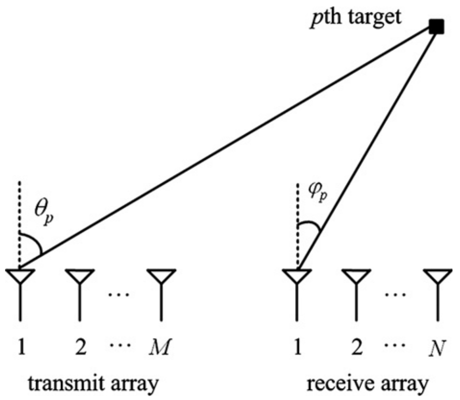

Fig. 1. Bistatic MIMO radar scenario.

another ESPRIT based method is presented in [12]. A polynomial root finding approach is proposed in [13]. The propagator method (PM) based method is given in [14] with lower computational cost but performance deterioration in low signal-to-noise-ratio (SNR) case than ESPRIT based methods. We can see that most of the existing methods are based on subspace estimation. They all require stacking the matched filter output into one structured matrix, and estimate the signal/noise subspace by SVD of this matrix or EVD of its covariance matrix. In fact, the matched filter output of a bistatic MIMO radar is multidimensional, and the traditional SVD/EVD based subspace estimate method does not make use of its inherent structure, which results in a significant performance loss in the parameter estimation.

In this paper, we proposed a new subspace estimation algorithm to improve the DOD and DOA estimation performance for bistatic MIMO radars. According to the multidimensional structure, multi-SVD [15,16] can be used. First, we formulate the matched filter output to a 3-order tensor, named measurement tensor. Then the signal subspace is estimated by multi-SVD of the matrix unfoldings of this measurement tensor or its covariance tensor. Simulation results validate that the proposed algorithm can yield more accurate estimation of the signal subspace than traditional methods, which results in better DOD–DOA performance when it is used to the subspace based parameter estimation methods, such as 2-D MUSIC and ESPRIT.

This paper is organized as follows. The signal model of the bistatic MIMO radar is described in Section 2. Section 3 presents the new multi-SVD based subspace estimation algorithm, and applies it to 2-D MUCISC and ESPRIT to estimate DOD–DOA. The computational complexity of the method is evaluated in Section 4. Section 5 gives some simulation results and compares the performance of the proposed method with the existing ones. Section 6 concludes the paper. The analytical performance evaluation of the proposed multi-SVD based subspace estimation algorithm is discussed in Appendix A.

Notations: we use the superscripts $(\cdot)^{\mathrm{T}}$,$(\cdot)^{\mathrm{H}}$, $(\cdot)^{*}$,$(\cdot)^{-1}$and$(\cdot)^{\dagger}$ for transposition, conjugate transposition, complex conjugate, matrix inversion and matrix Moore–Penrose pseudo-inverse, respectively. $\mathbf{I}_M$ is an $M \times M$ identity matrix.$\otimes$ and $\oplus$ symbolize the Kronecker product and Khatri–Rao product (column-wise Kronecker product), respectively. $||\cdot||_{\mathrm{F}}$ denotes matrix Frobenius norm. $\overline{\mathbf{A}}$ denotes the estimation of $\mathbf{A}$. diag $(\mathbf{a})$ forms a diagonal matrix that holds the entries of $\mathbf{a}$ on its diagonal. Angle (a) stands for the phase of a. vec $(\mathbf{A})$ builds a vector $\mathbf{a}$ by stacking the individual columns of the matrix $\mathbf{A} \in \mathbb{C}^{M \times N}$ one after each other, i.e., $(\mathbf{a})_{(n-1)M+m} = (\mathbf{A})_{m,n}$.

2. Signal model

Consider a narrowband bistatic MIMO radar with M-element transmit array and$N$-element receive array, both of which are half-wavelength spaced uniform linear arrays (ULA). Assume that there are P non-coherent targets located at some interested range cell in far-field. The p th target is located at (θ_p,φ_p), where θ_p is the angle of the p th target with respect to the transmit array, i.e., DOD, and φ_p is the angle with respect to the receive array, i.e., DOA. The bistatic MIMO radar scenario is shown in Fig. 1. The output of the nth receive antenna in the qth pulse is

$$\mathbf{x}_{n,q} = \sum_{p=1}^{P} \beta_{p,q} e^{j2\pi f_{dp} q T_{\mathrm{r}}} b_n(\varphi_p) \mathbf{a}^{\mathrm{T}}(\theta_p)\mathbf{S} + \mathbf{z}_{n,q} \tag{1}$$

where $\beta_{p,q}$ is the reflection coefficient of the pth target in the qth pulse, f_{dp} is the Doppler shift of the pth target, T_{r} is the pulse repetition interval, $\mathbf{a}(\theta_p) = [1, e^{j\pi \sin\theta_p}, \cdots, e^{j\pi(M-1)\sin\theta_p}]^{\mathrm{T}}$ is the transmit steering vector, and $b_n(\varphi_p)$ is the nth element of the receive steering vector $\mathbf{b}(\varphi_p) = [1, e^{j\pi \sin\varphi_p}, \cdots, e^{j\pi(N-1)\sin\varphi_p}]^{\mathrm{T}}$.$\mathbf{S} = [\mathbf{s}_1, \cdots, \mathbf{s}_M]^{\mathrm{T}} \in \mathbb{C}^{M \times L}$ is the matrix including M orthogonal narrowband transmit signals, L is the number of samples per pulse. $\mathbf{z}_{n,q}$ is the noise term for the qth pulse, $q = 1, 2, \cdots, Q$, and Q is the number of pulses during a coherent processing interval (CPI). The received signal of the qth pulse can be expressed as

$$\mathbf{X}_q = [\mathbf{x}_{1,q}^{\mathrm{T}}, \cdots, \mathbf{x}_{N,q}^{\mathrm{T}}]^{\mathrm{T}} = \mathbf{B}\mathbf{\Lambda}_q \mathbf{A}^{\mathrm{T}}\mathbf{S} + \mathbf{Z}_q \tag{2}$$

where $\mathbf{A} = [\mathbf{a}(\theta_1), \cdots, \mathbf{a}(\theta_P)]$ and $\mathbf{B} = [\mathbf{b}(\varphi_1), \cdots, \mathbf{b}(\varphi_P)]$ are the transmit array manifold and receive array manifold, respectively. $\mathbf{\Lambda}_q$=diag $(\mathbf{c}_q)$ with $\mathbf{c}_q = [\beta_{1,q} e^{j2\pi f_{d1} q T_{\mathrm{r}}}, \cdots, \beta_{P,q} e^{j2\pi f_{dP} q T_{\mathrm{r}}}]$ and $\mathbf{Z}_q = [\mathbf{z}_{1,q}^{\mathrm{T}}, \cdots, \mathbf{z}_{N,q}^{\mathrm{T}}]^{\mathrm{T}}$. The matched filter output of the qth pulse is

$$\mathbf{Y}_q = \mathbf{B}\mathbf{\Lambda}_q \mathbf{A}^{\mathrm{T}} + \mathbf{E}_q \tag{3}$$

where $\mathbf{Y}_q = \mathbf{X}_q \mathbf{S}^{\mathrm{H}}$, $\mathbf{E}_q = \mathbf{Z}_q \mathbf{S}^{\mathrm{H}}$. Let $\mathbf{y}_q$=vec$(\mathbf{Y}_q)$ and stack $\mathbf{y}_q$ one after another, we have

$$\mathbf{Y} = [\mathbf{y}_1, \cdots, \mathbf{y}_Q] = (\mathbf{A} \oplus \mathbf{B})\mathbf{C}^{\mathrm{T}} + \mathbf{E} \tag{4}$$

where $\mathbf{C}^{\mathrm{T}} = [\mathbf{c}_1^{\mathrm{T}}, \cdots, \mathbf{c}_Q^{\mathrm{T}}]$, $\mathbf{E} = [\mathbf{e}_1, \cdots, \mathbf{e}_Q]$, and $\mathbf{e}_q$=vec$(\mathbf{E}_q)$.

3. Improve DOD–DOA estimation using multi-SVD

In the subspace based DOD–DOA estimate methods, e.g., 2-D MUSIC [8] and ESPRIT [10], the signal/noise subspace can be determined by the following two ways. (1) Let the estimated signal subspace $\overline{\mathbf{U}_{\mathrm{s}}}$ be the left singular vectors of $\mathbf{Y}$ associated with the P significant singular values, and let the estimated noise subspace $\overline{\mathbf{U}}_{\mathrm{n}}$

be the rest $(MN-P)$ left singular vectors. (2) Let $\overline{\mathbf{U}}_s$ contain the eigenvectors of the covariance matrix $\mathbf{R}=1/Q\ \mathbf{Y}\mathbf{Y}^{\mathrm{H}}$ associated with the P significant eigenvalues and $\overline{\mathbf{U}}_n$ be the rest $(MN-P)$ eigenvectors. The later method is particularly efficient in the case that the number of pulses is large, i.e., $Q>MN$.

The above two classical methods both require stacking the matched filter output into one structured matrix, which discards the inherent multidimensional structure of measurements. In the following text, taking the multi-dimensional structure in mind, we present a novel multi-SVD based approach to improve subspace estimation accuracy. Furthermore the improved subspace estimation is used to the classical methods, i.e., 2-D MUSIC and ESPRIT, to improve the DOD and DOA performance.

3.1. Multi-SVD based subspace estimation

First, we introduce several tensor operations, which are consistent with [15,16].

Definition 1. The n-mode matrix unfolding of an N-order tensor $\boldsymbol{X}\in\mathbb{C}^{I_1\times I_2\times\cdots\times I_N}$, denoted by $\boldsymbol{X}_{(n)}\in\mathbb{C}^{I_n\times(I_{n+1}\cdots I_N I_1\cdots I_{n-1})}$, contains the $(i_1,i_2,\cdots i_N)$th element of $\boldsymbol{X}$ at the position (i_n,j), where $j=1+\sum_{k=1,k\neq n}^{N}(i_k-1)J_k$ with $J_k=\prod_{m=1,m\neq n}^{k-1}I_m$. On the contrary, given $\boldsymbol{X}_{(n)}$, $\boldsymbol{X}$ is constructed.

Definition 2. The n-mode product of a tensor $\boldsymbol{X}\in\mathbb{C}^{I_1\times I_2\times\cdots\times I_N}$ and a matrix $\mathbf{A}\in\mathbb{C}^{J_n\times I_n}$ is denoted as $\boldsymbol{Y}=\boldsymbol{X}\times_n\mathbf{A}$ where $\boldsymbol{Y}\in\mathbb{C}^{I_1\times I_2\times\cdots\times I_{n-1}\times J_n\times I_{n+1}\times\cdots\times I_N}$ and $y_{i_1,i_2,\cdots,i_{n-1},j_n,i_{n+1},\cdots,i_N}=\sum_{i_n=1}^{I_n}x_{i_1,i_2,i_{n-1},i_n,i_{n+1},\cdots,i_N}a_{j_n,i_n}$. The mode product satisfies the following properties [16]:

$$\boldsymbol{X}\times_m\mathbf{A}\times_n\mathbf{B}=\boldsymbol{X}\times_n\mathbf{B}\times_m\mathbf{A},\ \text{where } m\neq n \tag{5}$$

$$\boldsymbol{X}\times_n\mathbf{A}\times_n\mathbf{B}=\boldsymbol{X}\times_n(\mathbf{B}\mathbf{A}) \tag{6}$$

$$\begin{aligned}&[\boldsymbol{X}\times_1\mathbf{A}_1\times_2\mathbf{A}_2\times\cdots\times_K\mathbf{A}_K]_{(n)}\\&=\mathbf{A}_n\cdot\boldsymbol{X}_{(n)}\cdot[\mathbf{A}_{n+1}\otimes\mathbf{A}_{n+2}\cdots\otimes\mathbf{A}_K\otimes\mathbf{A}_1\cdots\otimes\mathbf{A}_{n-1}]^{\mathrm{T}}\end{aligned} \tag{7}$$

Definition 3. Multilinear SVD (Multi-SVD) of an N-way tensor $\boldsymbol{X}\in\mathbb{C}^{I_1\times I_2\times\cdots\times I_N}$ is given by $\boldsymbol{X}=\boldsymbol{C}\times_1\mathbf{U}_1\times_2\mathbf{U}_2\times_3\cdots\times_N\mathbf{U}_N$ where $\mathbf{U}_n\in\mathbb{C}^{I_n\times I_n}$ is the unitary matrix of the n-mode singular vectors with the SVD $\{\boldsymbol{X}_{(n)}=\mathbf{U}_n\boldsymbol{\Sigma}_n\mathbf{V}_n^{\mathrm{H}}\}_{n=1}^{N}$, $\boldsymbol{C}\in\mathbb{C}^{I_1\times I_2\times\cdots\times I_N}$, is the core tensor which satisfies the all orthogonality conditions [16], which means that two sub-tensors $\boldsymbol{C}_{i_n=\alpha}$ and $\boldsymbol{C}_{i_n=\beta}$ are orthogonal for all possible values of n, α and β subject to $\alpha\neq\beta$. Meanwhile, the core tensor can be written as [16] $\boldsymbol{C}=\boldsymbol{X}\times_1\mathbf{U}_1^{\mathrm{H}}\times_2\mathbf{U}_2^{\mathrm{H}}\times_3\cdots\times_N\mathbf{U}_N^{\mathrm{H}}$.

Using definition 1, we can construct a 3-order measurement tensor $\boldsymbol{Y}\in\mathbb{C}^{M\times N\times Q}$ from the matched filter output $\mathbf{Y}$ in (4) with $\boldsymbol{Y}_{(3)}=\mathbf{Y}^{\mathrm{T}}$. This 3-order tensor can be recognized as a data cube given in Fig. 2, and its matrix unfoldings consist of the slices of the cube along different directions. For example, $\boldsymbol{Y}_{(3)}$ is formed by concatenating

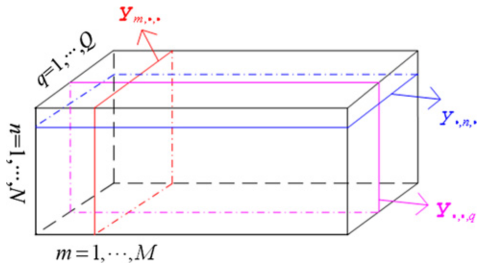

Fig. 2. Data cube of the 3-order measurement tensor and its matrix slices.

Q consecutive $M\times N$ matrix slices by fixing the third index along the pulse direction to successive values $q=1,2,\cdots,Q$.

3.1.1. Direct measurement tensor approach

In this subsection, we consider the case that MN is larger than Q, i.e., $MN>Q$. The signal subspace is estimated by direct processing on the measurement tensor $\boldsymbol{Y}$. The multi-SVD of $\boldsymbol{Y}\in\mathbb{C}^{M\times N\times Q}$ is given by

$$\boldsymbol{Y}=\overline{\boldsymbol{C}}\times_1\overline{\mathbf{U}}_1\times_2\overline{\mathbf{U}}_2\times_3\overline{\mathbf{U}}_3 \tag{8}$$

where $\overline{\mathbf{U}}_i$ is the left singular vectors of the i-mode matrix unfolding of $\boldsymbol{Y}$ as $\{\boldsymbol{Y}_{(i)}=\overline{\mathbf{U}}_i\overline{\boldsymbol{\Sigma}}_i\overline{\mathbf{V}}_i^{\mathrm{H}}\}_{i=1}^{3}$, and $\overline{\boldsymbol{C}}$ denotes the corresponding core tensor. Then we define a subspace tensor

$$\boldsymbol{P}=\overline{\boldsymbol{C}}_s\times_1\overline{\mathbf{U}}_{1s}\times_2\overline{\mathbf{U}}_{2s} \tag{9}$$

where $\overline{\mathbf{U}}_{is}$ contains the column vectors of $\overline{\mathbf{U}}_i$ corresponding to the significant P singular values, and $\overline{\boldsymbol{\Sigma}}_{is}$ is a diagonal matrix with the largest P singular values on its diagonal, where i=1, 2 and 3. $\overline{\boldsymbol{C}}_s$ stands for the signal component of $\overline{\boldsymbol{C}}$. Insertion of $\overline{\boldsymbol{C}}_s=\boldsymbol{Y}\times_1\overline{\mathbf{U}}_{1s}^{\mathrm{H}}\times_2\overline{\mathbf{U}}_{2s}^{\mathrm{H}}\times_3\overline{\mathbf{U}}_{3s}^{\mathrm{H}}$ into (9) gives

$$\boldsymbol{P}=\boldsymbol{Y}\times_1(\overline{\mathbf{U}}_{1s}\overline{\mathbf{U}}_{1s}^{\mathrm{H}})\times_2(\overline{\mathbf{U}}_{2s}\overline{\mathbf{U}}_{2s}^{\mathrm{H}})\times_3\overline{\mathbf{U}}_{3s}^{\mathrm{H}} \tag{10}$$

Then the signal subspace is given by $\overline{\mathbf{U}}_{\mathrm{simp}}=[\boldsymbol{P}_{(3)}]^{\mathrm{T}}$, using (7) we have

$$\overline{\mathbf{U}}_{\mathrm{simp}}=[\boldsymbol{P}_{(3)}]^{\mathrm{T}}=[(\overline{\mathbf{U}}_{1s}\overline{\mathbf{U}}_{1s}^{\mathrm{H}})\otimes(\overline{\mathbf{U}}_{2s}\overline{\mathbf{U}}_{2s}^{\mathrm{H}})]\mathbf{Y}\overline{\mathbf{U}}_{3s}^{*} \tag{11}$$

The relationship between $\overline{\mathbf{U}}_s$ and $\overline{\mathbf{U}}_{\mathrm{simp}}$ is discussed as follows. In the classical method, the estimated signal subspace can be determined by truncating SVD of $\mathbf{Y}$ as $\mathbf{Y}\approx\overline{\mathbf{U}}_s\overline{\mathbf{D}}_s\overline{\mathbf{V}}_s^{\mathrm{H}}$, insertion of it into (11) gives

$$\overline{\mathbf{U}}_{\mathrm{simp}}=[(\overline{\mathbf{U}}_{1s}\overline{\mathbf{U}}_{1s}^{\mathrm{H}})\otimes(\overline{\mathbf{U}}_{2s}\overline{\mathbf{U}}_{2s}^{\mathrm{H}})]\overline{\mathbf{U}}_s\overline{\mathbf{D}}_s\overline{\mathbf{V}}_s^{\mathrm{H}}\overline{\mathbf{U}}_{3s}^{*}\overline{\boldsymbol{\Sigma}}_{3s}^{-1} \tag{12}$$

Here we add the inverse of the diagonal matrix of 3-mode singular values $\overline{\boldsymbol{\Sigma}}_{3s}$. Note this scaling does not affect the signal subspace. This normalization is performed only to simplify the notation and make the relationship between $\overline{\mathbf{U}}_s$ and $\overline{\mathbf{U}}_{\mathrm{simp}}$ more clearly. Because $\boldsymbol{Y}_{(3)}=\overline{\mathbf{U}}_{3s}\overline{\boldsymbol{\Sigma}}_{3s}\overline{\mathbf{V}}_{3s}^{\mathrm{H}}$ and $\mathbf{Y}=[\boldsymbol{Y}_{(3)}]^{\mathrm{T}}$, we have $\overline{\mathbf{U}}_{3s}^{*}=\overline{\mathbf{V}}_s$ and $\overline{\mathbf{D}}_s=\overline{\boldsymbol{\Sigma}}_{3s}$. Then (12) is rewritten as

$$\overline{\mathbf{U}}_{\mathrm{simp}}=[(\overline{\mathbf{U}}_{1s}\overline{\mathbf{U}}_{1s}^{\mathrm{H}})\otimes(\overline{\mathbf{U}}_{2s}\overline{\mathbf{U}}_{2s}^{\mathrm{H}})]\overline{\mathbf{U}}_s \tag{13}$$

Eq. (13) describes the relationship between $\overline{\mathbf{U}}_s$ and $\overline{\mathbf{U}}_{\mathrm{simp}}$, in which $\overline{\mathbf{U}}_{\mathrm{simp}}$ stems from the projection onto the Kronecker product of the space spanned by 1-mode vectors $\overline{\mathbf{U}}_{1s}\overline{\mathbf{U}}_{1s}^{H}$ and the space spanned by 2-mode vectors $\overline{\mathbf{U}}_{2s}\overline{\mathbf{U}}_{2s}^{H}$.

In the absence of noise or the number of targets is larger than the number of transmit antennas and the number of receive antennas,$\overline{\mathbf{U}}_{simp}$ contains a basis for the signal subspace exactly in the same way as $\overline{\mathbf{U}}_{s}$ does, because in these two cases $\overline{\mathbf{U}}_{1s}\overline{\mathbf{U}}_{1s}^{H}$ and $\overline{\mathbf{U}}_{2s}\overline{\mathbf{U}}_{2s}^{H}$ are both identify matrices. The proposed multi-SVD approach yields the same result as the classical SVD method. In fact, $\overline{\mathbf{U}}_{1s}$ and $\overline{\mathbf{U}}_{2s}$ span the same signal subspace as the transmit array manifold **A** and receive array manifold **B** in the noise-free case, respectively.

In the presence of noise, the estimated basis of the signal subspace given by $\overline{\mathbf{U}}_{simp}$ differs from the one given by $\overline{\mathbf{U}}_{s}$ if a finite number of pulses is available, and the former yields more accurate subspace estimation. The reason for this improvement is that through multi-SVD of the matrix unfoldings of the measurement tensor, the structure inherent in the multidimensional measurements is exploited. Using the traditional SVD approach, this structure cannot be captured. Our method can filter out noise in each mode of the measurement tensor separately, which results in enhanced noise suppression.

The analytical performance evaluation of the multi-SVD based subspace estimation algorithm is discussed in Appendix A, in which we extend the first order perturbation analysis of SVD based subspace estimation to our multi-SVD case.

3.1.2. Covariance tensor approach

Here we address the case that MN is equal to or smaller than Q, i.e., $MN \le Q$. Define a 4-order tensor, named sample covariance tensor, and express it as

$$\boldsymbol{R} = \boldsymbol{Y} \bullet \boldsymbol{Y}^{*} \tag{14}$$

where $\boldsymbol{R} \in \mathbb{C}^{M\times N\times M\times N}$ and $(\boldsymbol{R})_{m,n,k,l} = 1/Q \cdot \sum_{q=1}^{Q} y_{m,n,q} y^{*}_{k,l,q}$, $m,k = 1,\cdots,M,n,l = 1,\cdots,N$. It is clear that $\boldsymbol{R}$ is an Hermitian tensor, i.e.,$(\boldsymbol{R})_{m,n,p,q} = (\boldsymbol{R})^{*}_{p,q,m,n}$. The multi-SVD of $\boldsymbol{R}$ is written as

$$\boldsymbol{R} = \overline{\boldsymbol{C}} \times_1 \overline{\mathbf{U}}_1 \times_2 \overline{\mathbf{U}}_2 \times_3 \overline{\mathbf{U}}_3 \times_4 \overline{\mathbf{U}}_4 \tag{15}$$

where $\overline{\mathbf{U}}_i$ is the left singular vectors of the i-mode matrix unfolding of $\boldsymbol{R}$ as $\{\boldsymbol{R}_{(i)} = \overline{\mathbf{U}}_i \overline{\boldsymbol{\Sigma}}_i \overline{\mathbf{V}}_i^{H}\}_{i=1}^{4}$, and $\overline{\boldsymbol{C}}$ denotes the corresponding core tensor. Then we define a covariance subspace tensor

$$\boldsymbol{H} = \overline{\boldsymbol{C}}_s \times_1 \overline{\mathbf{U}}_{1s} \times_2 \overline{\mathbf{U}}_{2s} \times_3 \overline{\mathbf{U}}_{3s} \times_4 \overline{\mathbf{U}}_{4s} \tag{16}$$

where $\overline{\mathbf{U}}_{is}$ contains the column vectors of $\overline{\mathbf{U}}_i$ corresponding to the significant P singular values, and $\overline{\boldsymbol{C}}_s$ stands for the signal components of $\overline{\boldsymbol{C}}$. Substituting $\overline{\boldsymbol{C}}_s = \boldsymbol{R} \times_1 \mathbf{U}_{1s}^{H} \times_2 \mathbf{U}_{2s}^{H} \times_3 \mathbf{U}_{3s}^{H} \times_4 \mathbf{U}_{4s}^{H}$ into (16) yields

$$\boldsymbol{H} = \boldsymbol{R} \times_1 (\overline{\mathbf{U}}_{1s}\overline{\mathbf{U}}_{1s}^{H}) \times_2 (\overline{\mathbf{U}}_{2s}\overline{\mathbf{U}}_{2s}^{H}) \times_3 (\overline{\mathbf{U}}_{3s}\overline{\mathbf{U}}_{3s}^{H}) \times_4 (\overline{\mathbf{U}}_{4s}\overline{\mathbf{U}}_{4s}^{H}) \tag{17}$$

According to (14), we can find the relationship between the covariance matrix $\mathbf{R} = 1/Q \cdot \mathbf{Y}\mathbf{Y}^{H}$ and covariance tensor $\boldsymbol{R}$. $\mathbf{R}$ is obtained by letting the first 2 indices vary along the columns (the 2nd index is the faster, then index 1) and the last 2 indices along the rows (in the same order) of $\boldsymbol{R}$. Using the same way, we can form a new covariance matrix $\mathbf{R}_{imp}$ from the covariance subspace tensor $\boldsymbol{H}$, which can be written as

$$\mathbf{R}_{imp} = [(\overline{\mathbf{U}}_{1s}\overline{\mathbf{U}}_{1s}^{H}) \otimes (\overline{\mathbf{U}}_{2s}\overline{\mathbf{U}}_{2s}^{H})]\mathbf{R}[(\overline{\mathbf{U}}_{3s}\overline{\mathbf{U}}_{3s}^{H}) \otimes (\overline{\mathbf{U}}_{4s}\overline{\mathbf{U}}_{4s}^{H})]^{*} \tag{18}$$

Because $\boldsymbol{R}$ is an Hermitian tensor, we have $\overline{\mathbf{U}}_{1s} = \overline{\mathbf{U}}_{3s}^{*}, \overline{\mathbf{U}}_{2s} = \overline{\mathbf{U}}_{4s}^{*}$. This allows us to compute the signal subspace via EVD of $\mathbf{R}_{imp}$, and let $\overline{\mathbf{U}}_{simp}$ contain the eigenvectors corresponding to the dominant P eigenvalues.

Equivalent of the direct measurement tensor approach and covariance tensor approach is proved as follows. In the classical method, the estimated signal subspace can be determined by truncating EVD of $\mathbf{R} = 1/Q \cdot \mathbf{Y}\mathbf{Y}^{H}$, i.e., $\mathbf{R} \approx \overline{\mathbf{U}}_s \overline{\mathbf{D}}_s \overline{\mathbf{U}}_s^{H}$. Inserting it into (18) yields

$$\mathbf{R}_{imp} = \{[(\overline{\mathbf{U}}_{1s}\overline{\mathbf{U}}_{1s}^{H}) \otimes (\overline{\mathbf{U}}_{2s}\overline{\mathbf{U}}_{2s}^{H})]\overline{\mathbf{U}}_s\}\overline{\mathbf{D}}_s\{[(\overline{\mathbf{U}}_{3s}\overline{\mathbf{U}}_{3s}^{H}) \otimes (\overline{\mathbf{U}}_{4s}\overline{\mathbf{U}}_{4s}^{H})]^{T}\overline{\mathbf{U}}_s\}^{H} \tag{19}$$

Considering $\overline{\mathbf{U}}_{1s} = \overline{\mathbf{U}}_{3s}^{*}, \overline{\mathbf{U}}_{2s} = \overline{\mathbf{U}}_{4s}^{*}$, after EVD of $\mathbf{R}_{imp}$, we have

$$\overline{\mathbf{U}}_{simp} = [(\overline{\mathbf{U}}_{1s}\overline{\mathbf{U}}_{1s}^{H}) \otimes (\overline{\mathbf{U}}_{2s}\overline{\mathbf{U}}_{2s}^{H})]\overline{\mathbf{U}}_s \tag{20}$$

It is easy to show that in the noiseless case $\overline{\mathbf{U}}_{1s}$ and $\overline{\mathbf{U}}_{2s}$ span the same signal subspace as the transmit array manifold **A** and receive array manifold **B**, respectively. Thus (13) and (20) are equivalent.

3.2. DOD–DOA estimation

We summarize two classical subspace based DOD and DOA estimation algorithms, i.e., 2-D MUSIC [8] and ESPRIT [10], only replacing the traditional SVD/EVD based subspace estimation by the proposed multi-SVD based subspace estimation. The DOD–DOA can be estimated by the 2-D MUSIC spectrum peak searching function [8]

$$P_{MUSIC}(\theta,\varphi) = \frac{1}{[\mathbf{a}(\theta) \otimes \mathbf{b}(\varphi)]^{H}\mathbf{R}_n[\mathbf{a}(\theta) \otimes \mathbf{b}(\varphi)]} \tag{21}$$

where $\mathbf{R}_n = \mathbf{I}_{MN} - \overline{\mathbf{U}}_{so}\overline{\mathbf{U}}_{so}^{H}$, where $\overline{\mathbf{U}}_{so}$ is the orthogonal basis of $\overline{\mathbf{U}}_{simp}$ for the multi-SVD method and $\overline{\mathbf{U}}_{s}$ for the traditional SVD/EVD method.

To use the ESPRIT based method in [10], we need construct another signal subspace $\overline{\mathbf{U}}'_{simp}$ from $\overline{\mathbf{U}}_{simp}$. It has been shown [17] that $\mathbf{A}_{tr}=\mathbf{A}\oplus\mathbf{B}$ is row equivalent to $\mathbf{A}_{rt}=\mathbf{B}\oplus\mathbf{A}$, and there exists a transformation matrix $\mathbf{T} \in$ complexes;$^{MN\times MN}$ corresponding to the finite number of row interchanged operations such that $\mathbf{A}_{rt}=\mathbf{T}\mathbf{A}_{tr}$. Let $\overline{\mathbf{U}}'_{simp} = \mathbf{T}\overline{\mathbf{U}}_{simp}$, where $\overline{\mathbf{U}}'_{simp} \in \mathbb{C}^{MN\times P}$ is the signal subspace formed from $\overline{\mathbf{U}}_{simp}$ by the same row interchanged operations as $\mathbf{A}_{rt}$ is formed from $\mathbf{A}_{tr}$. In the noise-free case, the columns in $\overline{\mathbf{U}}_{simp}$ and $\overline{\mathbf{U}}'_{simp}$ span the same signal subspaces as the columns in $\mathbf{A}_{tr}$ and $\mathbf{A}_{rt}$, respectively [10]. Then let $\boldsymbol{\Psi}_t = \mathbf{U}_{t1}^{\dagger}\mathbf{U}_{t2}$, where $\mathbf{U}_{t1}$ and $\mathbf{U}_{t2}$ are the $N(M-1)\times P$ submatrices consisting of the first and the last $N(M-1)$ rows of $\overline{\mathbf{U}}_{simp}$, respectively. Let **G** and **D** are the eigenvector matrix and eigenvalue matrix of $\boldsymbol{\Psi}_t$.

Then the DOD of the pth target is estimated by

$$\overline{\theta}_p = \arcsin[\text{angle}(d_{p,p})/\pi] \tag{22}$$

where $d_{p,p}$ is the pth diagonal element of $\mathbf{D}$. To estimate the DOA paired with the estimated DOD from (22), introduce the matrix $\mathbf{W}_\mathrm{r} = \overline{\mathbf{U}}'_{\mathrm{simp}}\mathbf{G}$, and let $\mathbf{W}_{\mathrm{r}1}$ and $\mathbf{W}_{\mathrm{r}2}$ are the $M(N-1)\times P$ submatrices consisting of the first and the last $M(N-1)$ rows of $\mathbf{W}_\mathrm{r}$, respectively. Let $\mathbf{D}'$ be the eigenvalue matrix of $\mathbf{\Psi}_\mathrm{r} = \mathbf{W}_{\mathrm{r}1}^{\dagger}\mathbf{W}_{\mathrm{r}2}$, and then the estimated DOA of the pth target is given by

$$\overline{\varphi}_p = \arcsin[\text{angle}(d'_{p,p})/\pi] \tag{23}$$

where $d'_{p,p}$ is the pth diagonal element of $\mathbf{D}'$.

It should be pointed out that our method can be used to other subspace based algorithms to improve angle estimation performance, such as RD-MUSIC approach [8] and polynomial root finding approach [13].

4. Computational complexity

In order to compare the complexity for computation of the signal subspace, we have to know the complexity of SVD algorithm. Many SVD algorithms have been studied and their complexities differ [18]. Among them the orthogonal iteration approach is an efficient solution, which for an $I\times J$ matrix truncated to rank K has a complexity in order of $O(IJK)$. Considering this in mind, in $MN>Q$ case, the main computational cost of each approach is $O(MNQP)$ for the traditional method resulting from SVD of $\mathbf{Y}$, and $O(3MNQP)$ for our multi-SVD method resulting from three SVDs of matrix unfoldings of the measurement tensor $\boldsymbol{\mathcal{Y}}$. In $MN\le Q$ case, the main computational complexity of each approach is $O(M^2N^2P)$ for the traditional method resulting from EVD of the covariance matrix $\mathbf{R}$, and $O(4M^2N^2P)$ for our multi-SVD method resulting from four SVDs of matrix unfoldings of the covariance tensor $\boldsymbol{\mathcal{R}}$ and EVD of $\mathbf{R}_{\mathrm{imp}}$. It shows that the computational complexity is higher in the multi-SVD approach than in the traditional SVD/EVD approach but of the same order.

5. Simulation results

Some simulations are conducted to demonstrate the improvement of the proposed multi-SVD approach. The considered bistatic MIMO radar is composed of $M=10$ elements in transmit array and $N=10$ elements in receive array. Both the transmit array and receive array are half-wavelength spaced ULA arrays. The pulse repetition interval is $T_\mathrm{r}=50$ μs, and the number of samples per pulse is $L=512$. The mth transmitted waveform $\mathbf{s}_m$, i.e., the mth row of $\mathbf{S}$, is generated by $\mathbf{s}_m=(1+j)/\sqrt{2}\mathbf{h}_m$, where $\mathbf{h}_m$ is the mth row of the $L\times L$ Hadamard matrix. Three non-coherent targets are located at angles $\{\theta_p\}_{p=1}^3 = \{30^\circ,45^\circ,-40^\circ\}$, $\{\varphi_p\}_{p=1}^3=\{-10^\circ,5^\circ,30^\circ\}$, and Doppler shifts are $\{f_{\mathrm{d}p}\}_{p=1}^3=\{200,250,\ 300\}$Hz. The target reflection coefficient model is Swerling-II (the reflection coefficients are varying from pulse to pulse during a CPI), and the first two targets are correlated with a correlation coefficient $\rho=0.95$. The additive noise is assumed to be spatial white complex Gaussian process. We use direct measurement tensor approach in the case $MN<Q$ and the covariance tensor approach in the case $MN\ge Q$ to estimate the signal subspace in the proposed multi-SVD method. Three simulation cases are addressed to show the effectiveness of the proposed algorithm. The number of Monte Carlo trials is fixed at 500 for all cases.

Case 1:. We examine the accuracy of the estimated signal subspace via measuring root mean squares error (RMSE) of the estimated subspace, i.e., $||\mathbf{\Delta U}_\mathrm{s}||_\mathrm{F}$ and $||\mathbf{\Delta U}_{\mathrm{simp}}||_\mathrm{F}$ given in Appendix A. The empirical subspace estimation error per column is computed as [19].

$$\Delta\mathbf{u}_p = \overline{\mathbf{u}}_p\frac{\overline{\mathbf{u}}_p^{\mathrm{H}}\mathbf{u}_p}{\left|\overline{\mathbf{u}}_p^{\mathrm{H}}\mathbf{u}_p\right|}-\mathbf{u}_p,\ p=1,2,\cdots,P$$

where $\mathbf{\Delta u}_p$ is the pth column of $||\mathbf{\Delta U}_\mathrm{s}||_\mathrm{F}$ for the traditional SVD method and $||\mathbf{\Delta U}_{\mathrm{simp}}||_\mathrm{F}$ for our method, $\overline{\mathbf{u}}_p$ is the pth column of the estimated signal subspace $\overline{\mathbf{U}}_\mathrm{s}$ for the traditional SVD method and $\overline{\mathbf{U}}_{\mathrm{simp}}$ for our method, and $\mathbf{u}_p$ is the pth column of the true subspace $\mathbf{U}_\mathrm{s}$ which contains the left singular vectors of $(\mathbf{A}\oplus\mathbf{B})\mathbf{C}^\mathrm{T}$ associated with the largest three singular values. Fig. 3 plots the RMSEs of signal subspace estimation of SVD method and the proposed multi-SVD method with the number of pulses $Q=16$. It can be seen that the accuracy of our approach clearly outperforms that of the traditional SVD method with an improvement by a factor of 3.3. This improvement results from the fact that we exploit the multidimensional structure of the data, and process the matrix unfoldings of the measurement tensor 'jointly'. We know that our desired multidimensional signal obeys this unique property while the noise does not—this can be used to filter out more of the noise. This is something the traditional SVD of the stacked matrix representation does not exploit.

Moreover, in Fig. 3 we give the analytical performance of SVD method and multi-SVD method according to (A2) and (A6) in Appendix A. We observe a good fit between analytical results and empirical results, especially for higher SNRs.

Case 2:. Fig. 4 gives the probability of successful detection of different methods under $Q=16$. Successful detection requires that the absolute errors of DOD and DOA for

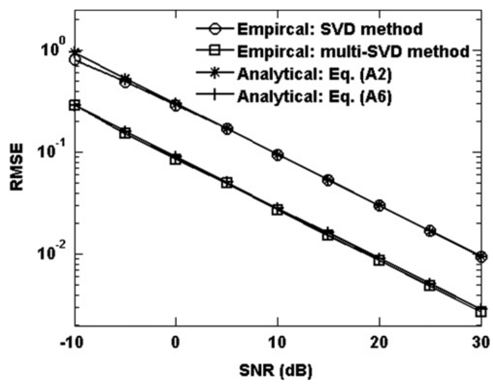

Fig. 3. RMSEs of the signal subspace estimation versus SNR.

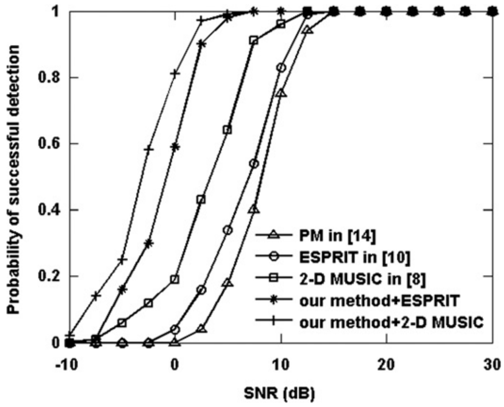

Fig. 4. Probability of successful detection versus SNR.

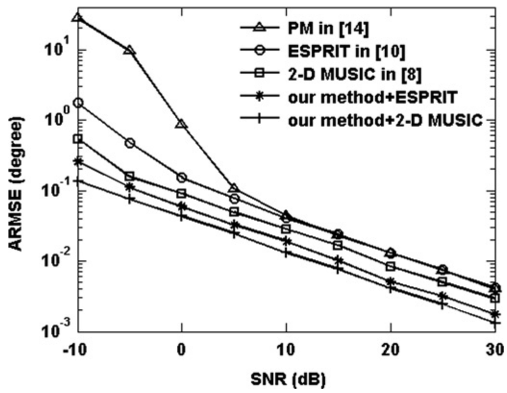

Fig. 5. ARMSEs of angle estimation versus SNR.

all three targets are within 0.1°. Additionally, for the comparison between all methods to be fair, the angular resolution of the 2-D MUSIC based techniques is fixed to 0.001°. Since scanning all possible pairs of angle (θ,φ) between $-90°$ and 90° with such a small angular step-size takes too long, we proceed as follows. The first round of scanning is done with a step size of 1°, to get a first localization of the three highest peaks. Then the estimation is refined individually for each target around those peaks in several rounds, to reach the final resolution of 0.001°. It can be seen from Fig. 4 that all methods exhibit a 100% successful detection at high SNR values. As the SNR decreases, the probability of successful detection starts dropping for each method at a certain point, known as SNR threshold, until it eventually becomes zero. The multi-SVD based 2-D MUSIC and ESPRIT have the lower SNR threshold than the corresponding SVD based methods [8,10], and the PM [14] has the highest SNR threshold. It is evident that the multi-SVD based methods outperform the SVD counterparts. This comes from the improved accuracy of subspace estimation in the multi-SVD method.

Case 3:. We address the angle performance of the proposed multi-SVD based algorithms, and compare them with the existing methods. The performance criterion used is the average root mean square error (ARMSE), averaged over all angles, all targets and all Monte Carlo trials, which is defined as

$$\text{ARMSE} = \sqrt{\frac{1}{2M_c P}\sum_{m=1}^{M_c}\sum_{p=1}^{P}(\overline{\theta}_{m,p}-\theta_p)^2+(\overline{\varphi}_{m,p}-\varphi_p)^2}$$

where M_c is the number of Monte Carlo trials, $\overline{\theta}_{m,p}$ and $\overline{\varphi}_{m,p}$ are the estimations of DOD and DOA for the pth target in the mth Monte Carlo trial, respectively.

The simulation results depicted in Fig. 5 provide a comparison of ARMSEs of different methods versus SNR with $Q=16$. It can be seen the proposed multi-SVD based methods have better angle performance than the corresponding SVD based approaches in [8,10]. This improvement results from the fact that in our approaches we take into account the special structure of multidimensional data while computing the signal subspace. This allows us to de-noise the measurements more efficiently, and gives more accurate estimation of the signal subspace, just as elaborated in Case 1. For subspace based spectrum estimation methods, such as MUSIC and ESPRIT, generally, better subspace means better angle performance. It can also be seen that the PM in [14] has the same performance as ESPRIT in [10] at a high SNR region, and has worse performance than the others. This conclusion is consistent with [14].

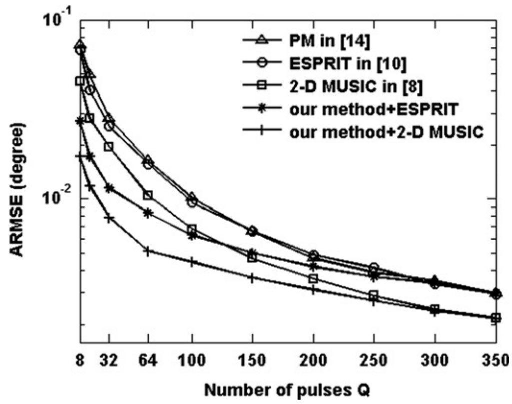

Fig. 6. ARMSEs of angle estimation versus the number of pulses.

Fig. 6 shows a comparison of ARMSEs of different approaches versus the number of pulses under SNR = 10 dB. It is indicated that the multi-SVD based methods have better angle performance than the corresponding SVD/EVD based methods in small pulse number case, and has nearly the same performance when Q is larger than 300. This shows that in larger pulse number case the estimated performance using traditional SVD/EVD is very close to that of the multi-SVD. The performance improvement is lost for large pulse number, and this may be caused by the averaging of the number of pulses. We have no better explanation yet why the performance does not improve in this case, and we are still investigating this issue further.

6. Conclusions

In this paper, a multi-SVD based subspace estimation method is proposed to improve the angle performance in bistatic MIMO radars. It shows the multi-SVD leads to improved signal subspace estimation, thereby resulting in better angle performance when it is applied to subspace based parameter estimation approaches such as 2-D MUSIC and ESPRIT, only at the cost of a little increasing computational complexity. This improvement results from the fact that the proposed method takes the special structure of the multidimensional data into account while computing the signal subspace based on multi-SVD of matrix unfoldings of the measurement tensor or its covariance tensor. This allows us to suppress the noise more efficiently. It should be pointed out that this advantage is obtained in case that the number of targets is less than the number of antennas in at least one of the transmit array and receive array and only a small number of pulses is available.

Acknowledgments

This work is supported by Ministry Pre-Research Foundation of China under Grant 9140A07010311BQ02 and Nanjing University of Science and Technology Research Funding under Grant 2010ZDJH05.

Appendix A

Here, we deduce the analytical performance evaluation of the proposed multi-SVD based subspace estimation algorithm by extending the first order perturbation analysis of SVD based subspace estimation to the multi-SVD case. Rewrite (4) as $\mathbf{Y}=\mathbf{Y}'+\mathbf{E}$, where $\mathbf{Y}'=(\mathbf{A}\oplus\mathbf{B})\mathbf{C}^{\mathrm{T}}$, $\mathbf{E}$ is the noise term. The SVD of $\mathbf{Y}'$ is expressed as

$$\mathbf{Y}' = \begin{bmatrix} \mathbf{U}_s & \mathbf{U}_n \end{bmatrix} \begin{bmatrix} \mathbf{\Sigma}_s & 0 \\ 0 & 0 \end{bmatrix} \begin{bmatrix} \mathbf{V}_s^{\mathrm{H}} \\ \mathbf{V}_n^{\mathrm{H}} \end{bmatrix} \tag{A1}$$

The first order perturbation of the true signal subspace $\mathbf{U}_s$ via SVD of the noisy data is given by [20]

$$\Delta\mathbf{U}_s = \overline{\mathbf{U}}_s - \mathbf{U}_s = \mathbf{U}_n\mathbf{U}_n^{\mathrm{H}}\mathbf{E}\mathbf{V}_s\mathbf{\Sigma}_s^{-1} \tag{A2}$$

Then we extend this conclusion to our multi-SVD method. Let the matrix unfoldings of the measurement tensor be $\mathbf{Y}_{(i)} = \mathbf{Y}'_{(i)} + \mathbf{E}_{(i)}$, and $\mathbf{Y}'_{(i)}$ denotes the noise-free term, and its SVD is

$$\mathbf{Y}'_{(i)} = \begin{bmatrix} \mathbf{U}_{is} & \mathbf{U}_{in} \end{bmatrix} \begin{bmatrix} \mathbf{\Sigma}_{is} & 0 \\ 0 & 0 \end{bmatrix} \begin{bmatrix} \mathbf{V}_{is}^{\mathrm{H}} \\ \mathbf{V}_{in}^{\mathrm{H}} \end{bmatrix}, i=1,2,3 \tag{A3}$$

Let $\overline{\mathbf{U}}_{is} = \mathbf{U}_{is} + \Delta\mathbf{U}_{is}$ and $\overline{\mathbf{W}}_i = \overline{\mathbf{U}}_{is}\overline{\mathbf{U}}_{is}^{\mathrm{H}}$, then we have

$$\begin{aligned}\overline{\mathbf{W}}_i &= (\mathbf{U}_{is}+\Delta\mathbf{U}_{is})(\mathbf{U}_{is}+\Delta\mathbf{U}_{is})^{\mathrm{H}} \\ &= \mathbf{W}_i + \mathbf{U}_{is}\Delta\mathbf{U}_{is}^{\mathrm{H}} + \Delta\mathbf{U}_{is}\mathbf{U}_{is}^{\mathrm{H}} + \Delta\mathbf{U}_{is}\Delta\mathbf{U}_{is}^{\mathrm{H}}\end{aligned} \tag{A4}$$

Since we are only interested in the first order perturbation analysis, the last term in (A4) can be neglected. Insertion of (A4) into (20) yields

$$\begin{aligned}\overline{\mathbf{U}}_{simp} &= (\overline{\mathbf{W}}_1 \otimes \overline{\mathbf{W}}_2)\overline{\mathbf{U}}_s \\ &= (\mathbf{W}_1 \otimes \mathbf{W}_2)\mathbf{U}_s + (\mathbf{W}_1 \otimes \mathbf{W}_2)\Delta\mathbf{U}_s \\ &\quad + [(\mathbf{U}_{1s}\Delta\mathbf{U}_{1s}^{\mathrm{H}} + \Delta\mathbf{U}_{1s}\mathbf{U}_{1s}^{\mathrm{H}}) \otimes \mathbf{W}_2]\mathbf{U}_s \\ &\quad + [\mathbf{W}_1 \otimes (\mathbf{U}_{2s}\Delta\mathbf{U}_{2s}^{\mathrm{H}} + \Delta\mathbf{U}_{2s}\mathbf{U}_{2s}^{\mathrm{H}})]\mathbf{U}_s\end{aligned} \tag{A5}$$

So the first order perturbation of $\mathbf{U}_{simp}=(\mathbf{W}_1\otimes\mathbf{W}_2)\mathbf{U}_s$ can be written as

$$\begin{aligned}\Delta\mathbf{U}_{simp} &= (\mathbf{W}_1 \otimes \mathbf{W}_2)\Delta\mathbf{U}_s + [(\mathbf{U}_{1s}\Delta\mathbf{U}_{1s}^{\mathrm{H}} + \Delta\mathbf{U}_{1s}\mathbf{U}_{1s}^{\mathrm{H}}) \otimes \mathbf{W}_2]\mathbf{U}_s \\ &\quad + [\mathbf{W}_1 \otimes (\mathbf{U}_{2s}\Delta\mathbf{U}_{2s}^{\mathrm{H}} + \Delta\mathbf{U}_{2s}\mathbf{U}_{2s}^{\mathrm{H}})]\mathbf{U}_s\end{aligned} \tag{A6}$$

where $\mathbf{W}_i = \mathbf{U}_{is}\mathbf{U}_{is}^{\mathrm{H}}$, $\Delta\mathbf{U}_{is} = \mathbf{U}_{in}\mathbf{U}_{in}^{\mathrm{H}}\mathbf{E}_{(i)}\mathbf{V}_{is}\mathbf{\Sigma}_{is}^{-1}$, $i=1,2$. $\mathbf{U}_s$ is given in (A1), $\Delta\mathbf{U}_s = \mathbf{V}_{3n}^{*}\mathbf{V}_{3n}^{\mathrm{T}}\mathbf{E}_{(3)}^{\mathrm{T}}\mathbf{U}_{3s}^{*}\mathbf{\Sigma}_{3s}^{-1}$ is consistent with (A2) because of $\mathbf{Y}' = (\mathbf{Y}'_{(3)})^{\mathrm{T}}$ and $\mathbf{U}_n = \mathbf{V}_{3n}^{*}, \mathbf{V}_s = \mathbf{U}_{3s}^{*}, \mathbf{\Sigma}_s = \mathbf{\Sigma}_{3s}$. Eq. (A6) gives the first order error of the estimated signal subspace for the proposed multi-SVD method.

References

[1] A. Haimovich, R. Blum, L. Cimini, MIMO radar with widely separated antennas, IEEE Signal Processing Magazine 25 (1) (2008) 116–129.
[2] J. Li, P. Stoica, MIMO radar with collocated antennas, IEEE Signal Processing Magazine 24 (5) (2007) 106–114.
[3] L.Z. Xu, J. Li, P. Stoica, Target detection and parameter estimation for MIMO radar system, IEEE Transactions on Aerospace and Electronic Systems 44 (30) (2008) 927–939.
[4] J. Dai, W. Xu, D. Zhao, Real-valued DOA estimation for uniform linear array with unknown mutual coupling, Signal Processing 92 (9) (2012) 2056–2065.
[5] K.N. Le, A new formula for the angle of arrival probability density function in mobile environment, Signal Processing 87 (6) (2007) 1314–1325.
[6] K.N. Le, On angle-of-arrival and time-of-arrival statistics of geometric scattering channels, IEEE Transactions on Vehicular Technology 58 (8) (2009) 4257–4264.
[7] H.D. Yan, J. Li, G.S. Liao, Multitarget identification and localization using bistatic MIMO radar systems, EURASIP Journal on Advances Signal Processing 8 (2) (2008) 1–8.
[8] X.F. Zhang, L.Y. Xu, L. Xu, D.Z. Xu, Direction of departure (DOD) and direction of arrival (DOA) estimation in MIMO radar with reduced dimension MUSIC, IEEE Communications Letters 14 (12) (2010) 1161–1163.
[9] D.F. Cheng, B.X. Cheng, G.D. Qin, Angle estimation using ESPRIT in MIMO radar, Electronics Letters 44 (12) (2008) 770–771.
[10] J.L. Chen, H. Gu, W.M. Su, Angle estimation using ESPRIT without pairing in MIMO radar, Electronics Letters 44 (24) (2008) 1422–1423.
[11] M. Jin, G.S. Liao, J. Li, Joint DOD and DOA estimation for bistatic MIMO radar, Signal Processing 89 (2) (2009) 244–251.
[12] J.L. Chen, H. Gu, W.M. Su, A new method for joint DOD and DOA estimation in bistatic MIMO radar, Signal Processing 90 (2) (2010) 714–718.
[13] M.L. Mencheikh, Y.D. Wang, H.Y. He, Polynomial root finding technique for joint DOA DOD estimation in bistatic MIMO radar, Signal Processing 90 (2) (2010) 2723–2730.
[14] Z.D. Zheng, J.Y. Zhang, Fast method for multi-target localization in bistatic MIMO radar, Electronics Letters 47 (2) (2011) 138–139.
[15] T.G. Kolda, B.W. Bader, Tensor decomposition and application, SIAM Review 51 (3) (2009) 455–500.
[16] L.D. Lathauwer, B.D. Moop, J. Vandewalle, A multilinear singular value decomposition, SIAM Journal on Matrix Analysis and Application 21 (4) (2000) 1253–1278.
[17] S.J. Leon, Linear Algebra With Applications, Prentice Hall, New Jersey, 2002.
[18] G.H. Golub, V.C.F. Loan, Matrix Computations, Johns Hopkins University Press, Baltimore, 1996.
[19] J. Liu, X.Q. Liu, X.L. Ma, First-order perturbation analysis of singular vectors in singular value decomposition, IEEE Transactions on Signal Processing 56 (7) (2008) 3044–3049.
[20] Z. Xu, Perturbation analysis for subspace decomposition with applications in subspace-based algorithms, IEEE Transactions on Signal Processing 50 (11) (2002) 2820–2830.